Interchromophoric Coupling in Oligo(*p*-phenylenevinylene)-Substituted Poly(propyleneimine) Dendrimers

Stefan C. J. Meskers,[†] Markus Bender,[‡] Jens Hübner,[‡] Yu. V. Romanovskii,[†,§] Michael Oestreich,[‡,||] Albertus P. H. J. Schenning,[⊥] E. W. Meijer,[⊥] and Heinz Bässler*[,†]

Institute of Physical Chemistry, Nuclear Chemistry and Macromolecular Chemistry, Philipps-University of Marburg, Hans Meerweinstrasse, D-35032 Marburg, Germany, Institute of Physics, Philipps-University of Marburg, Renthof 5, D-35032 Marburg, Germany, Institute of Spectroscopy, RAS, Troitsk 142092, Russian Federation, Institute of Solid State Physics, University Hannover, Appelstrasse 2, D-30167 Hannover, Germany, and Laboratory for Macromolecular and Organic Chemistry, Eindhoven University of Technology, P.O. Box 513 NL 5600MB Eindhoven, The Netherlands

Received: May 10, 2001; In Final Form: August 8, 2001

Poly(propyleneimine) dendrimers functionalized with oligo(*p*-phenylenevinylene) (OPV) end groups based on distyrylbenzene show fluorescence properties that depend on dendrimer generation and thereby on the number of end groups. The compounds are investigated using site-selective and time-resolved fluorescence methods. A red shift of the low-temperature emission spectrum is observed with increasing dendrimer generation. This is accompanied by changes in the shape of the lowest absorption band of the dendrimers. Results are interpreted in terms of rapid migration of electronic excitation energy among the OPV units. We find that coupling between the electronic motion on the OPV groups has to be taken into account to explain the magnitude of the red shift in emission. This implies that interchromophoric interactions are sufficiently strong to induce delocalization of the excitation over more than one chromophoric group. Experimental data indicate that off-diagonal disorder is large; i.e., excited-state interchromophoric interaction energies are given by a broad statistical distribution. The off-diagonal disorder is interpreted in terms of the flexible nature of the dendrimer, leading to a broad distribution of distances between the chromophoric end groups. A delayed emission component is observed for the dendrimers, but this component is absent for the isolated OPV unit. The delayed emission is attributed to excimer and/or exciplex formation within the dendrimer.

Introduction

The photophysical properties of π-conjugated polymers have been under intense investigation in the past decade, not in the least because of their promising technological applications. It is known that light emission from the polymer involves the lowest excited singlet state both in electro- and photogenerated luminescence.[1] For certain derivatives of poly(*p*-phenylenevinylene) (PPV) it has been observed that the probability per unit time for emission of a photon from the lowest excited state is reduced when the polymer is present as solid film in comparison to the polymer in dilute solution.[2] This led to the hypothesis that photoexcitations can exist as *inter*chain species, i.e., a species that is delocalized over more than one chain. A number of other studies have yielded evidence for interchain excitations and the associated interchain electronic interaction in films of π-conjugated polymers.[3]

It has also been realized that for the interchain species to exist, certain requirements in the relative geometrical orientations of neighboring chains on which the excitation residues have to be fulfilled. Most likely the chains have to be parallel and at a very short distance. The term "aggregate" has been used to describe a cluster of polymer chain (segments) fulfilling these geometrical requirements within a film of conjugated polymer.[4]

Films of π-conjugated polymer have a largely amorphous, disordered structure with the aggregate phase normally making up only a fraction of the total volume. The chains do not have a fixed length and conformational defects occurring along the chain are expected to limit the delocalization of electrons. Disorder in the packing of the chains will certainly also result in a spread in the excited-state interaction energies between the neighboring chains. It is well-known that such disorder induces localization of excitations.[5] It can therefore be expected that a large part of the states available for the excitations are strongly localized, most likely on a single chain (segment). Furthermore, the disorder results in a strong inhomogeneous broadening of the absorption band of the polymer. Photoexcitations can relax within the inhomogeneously broadened density of states by energy transfer to another chain segment with longer conjugation length.[6] Trapping of an excitation on an aggregate within the film is also a possible decay path. Altogether, this leads to a rather complex dynamical behavior.

Here we present photophysical studies on a model system for disordered clusters of π-conjugated molecules. We investigate poly(propyleneimine) dendrimers[7] of different generation, end capped with oligomers of (*p*-phenylenevinylene)[8] (OPV). The oligomer is a derivative of distyrylbenzene and bears alkoxy substituents (see Scheme 1). Various derivatives of distryryl-

* To whom correspondence should be addressed. Fax: +49-6421-28-28916. Phone: +49-6421-28-22190. E-mail: baessler@mailer.uni-marburg.de.

[†] Institute of Physical Chemistry, Nuclear Chemistry and Macromolecular Chemistry, Philipps-University of Marburg.

[‡] Institute of Physics, Philipps-University of Marburg.

[§] Institute of Spectroscopy, RAS.

[||] University Hannover.

[⊥] Eindhoven University of Technology.

10.1021/jp0117922 CCC: $20.00
Published on Web 10/12/2001

SCHEME 1

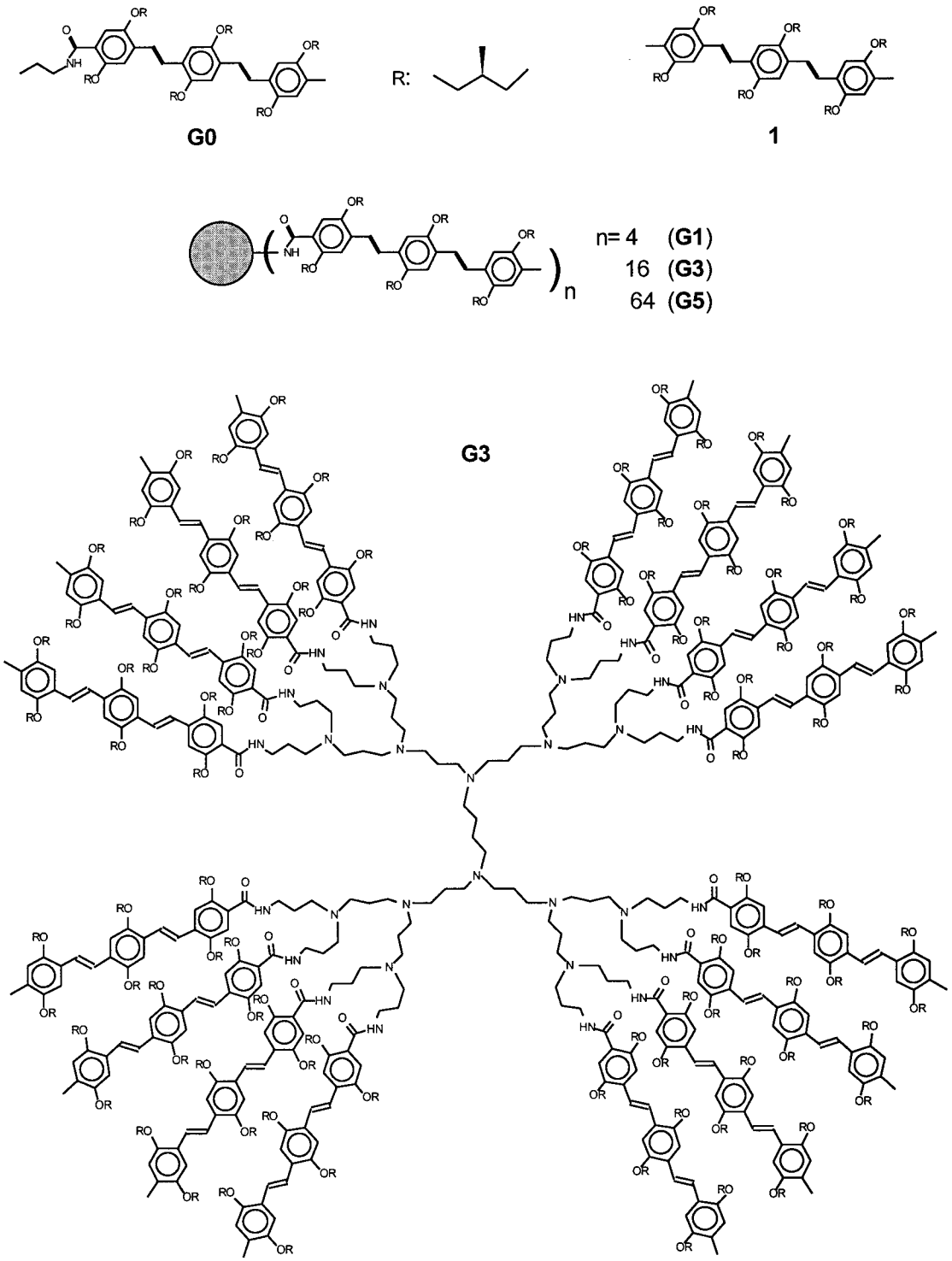

benzene (DSB) have been studied previously, and it is known that they can form (nanocrystalline) aggregates with spectroscopic properties differing from those of the solvated isolated molecule.[9] Studies on DSB dimers with a covalent paracyclophane linkage have indeed confirmed the electronic coupling between the molecules.[10−12] These studies have shown that this oligomer is a useful model compound to study the effect of interchain electronic coupling on the photophysical properties of π-conjugated materials. In combination with dendrimers of different generation, one has the possibility to bring together a well-defined number of OPV groups. The dendrimers used here are flexible, allowing for considerable positional disorder of the end groups. Therefore, one expects that the photophysical behavior may differ from that of a nanocrystalline aggregate of OPV molecules.

Several types of dendrimers functionalized with chromophoric groups[13] have been studied, especially in relation with directed transport of electronic energy within the macromolecule.[14] Studies of pyrene-functionalized poly(propyleneimine) dendrimers have shown that pyrene excimer formation can occur.[15] Excimer-like behavior could also be observed for dendrimers with peryleneimide chromophores.[16] Thus it seems that functionalized dendrimers are indeed useful model compounds to study photophysical processes.

In this study we use site-selective fluorescence (SSF) spectroscopy[17] to investigate the clusters of chromophores in the form of the OPV-substituted dendrimers. This method can be used to investigate energy relaxation in systems with an inhomogeneously broadened density of states and has been applied to π-conjugated molecules.[18] A narrow laser line is used to excite the species under study so that only electronic excited states in a narrow energy interval are initially populated. The fluorescence spectrum is recorded, and the excitation energy is then scanned through the absorption band. Applied to π-conjugated polymers at low temperature, the measurements have shown the existence of a "localization energy" for the excitations in the red tail of the absorption spectrum. Above this demarcation energy (E_{loc}), photoexcitations can relax by energy transfer to a neighboring chain (segment) with lower excitation energy. This results in an emission spectrum that is independent of the excitation energy E provided that $E > E_{loc}$. Below the localization energy, the probability for a photoexcitation to migrate during its lifetime to a site with even lower excitation energy is practically zero. This is because no states of lower energy are present in the close proximity of the excited chromophore. Hence fluorescence is observed from a photoselected ensemble of excited-state energy levels of which the mean energy and width are determined by the excitation energy used when $E < E_{loc}$.

Experimental Section

Site selective fluorescence spectra were measured at low temperature using a coldfinger cryostat (15 K). An excimer pumped dye laser (Lambda Physik) was used to excite the frozen solution and a multichannel CCD camera (Spectraview 2D, Instruments SA) in combination with a 0.27 m monochromator was used to detect and disperse the fluorescence. Time-resolved fluorescence spectra in the picosecond time range were collected using a streak camera (C6860, Hamamatsu) synchronized to the 80 MHz repetition frequency of the optical parametric oscillator pumped by a Ti:sapphire laser (Spectra Physics). With this instrument, picosecond time resolution can be achieved. Time-resolved fluorescence data in the nanosecond time domain were obtained using the excimer pumped dye laser (Lambda Physik) as excitation source and an optical multichannel analyzer (model 1460, Par) with a gatable intensified diode as detector. Absorption data were recorded with a lambda 9 spectrometer (Perkin-Elmer) in which a bath cryostat (Oxford Instruments). OPV-functionalized dendrimers were synthesized as described.[8]

Results

In Figure 1 low-temperature absorption and fluorescence spectra of the dendrimers **G0**, **G1**, **G3**, and **G5** are shown. At low temperature (100 K) in a 2MeTHF matrix, the absorption spectra show vibronic fine structure with a characteristic energy separation between the bands of about ~1400 cm^{-1}. At room temperature this fine structure is absent and only a broad featureless absorption band is observed.[8] This thermochromic behavior is characteristic for *p*-phenylenevinylene oligomers with alkoxy substituents.[19] At room temperature, the thermal energy is apparently large enough to induce torsional deformations of the π-system that influence the electron delocalization and, hence, the energy of the lowest excited state.[20] The absorption spectra show relatively small changes with dendrimer generation. This is further illustrated in Figure 2. Upon increasing the dendrimer generation, the ratio between the intensities of the first ("0−0") and second vibronic ("0−1") band changes in favor of the 0−1 band. Second, a low-energy tail appears for the higher dendrimers, associated with a broadening of the 0−0 absorption band. This may be further quantified by fitting a Gaussian curve to the low-energy side of the first vibronic transition. The width of the Gaussian fitted (σ_{abs}) is listed in Table 1 and increases with dendrimer generation. The fluorescence spectra obtained under nonselective excitation (λ_{exc} = 430 nm) are also illustrated in Figure 1; they show a substantial bathochromic shift with increasing number of end groups.

In Figure 3 fluorescence spectra for **G5** obtained with various excitation wavelengths are given. For excitation frequencies

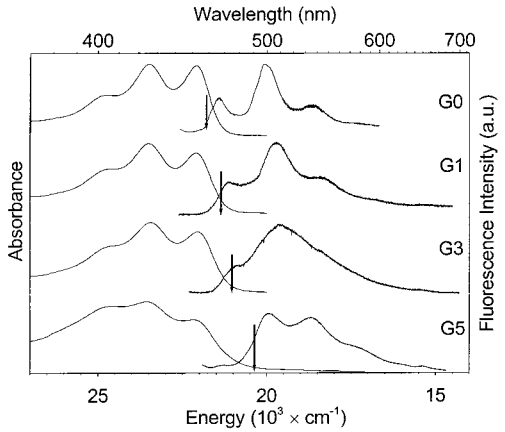

Figure 1. Absorption and fluorescence spectra of OPV3-modified propyleneimine dendrimers in 2-MeTHF. Absorption spectra were taken at T = 100 K and fluorescence spectra at T = 15 K. The arrows mark the localization energy as determined from SSF measurements (see Figure 4).

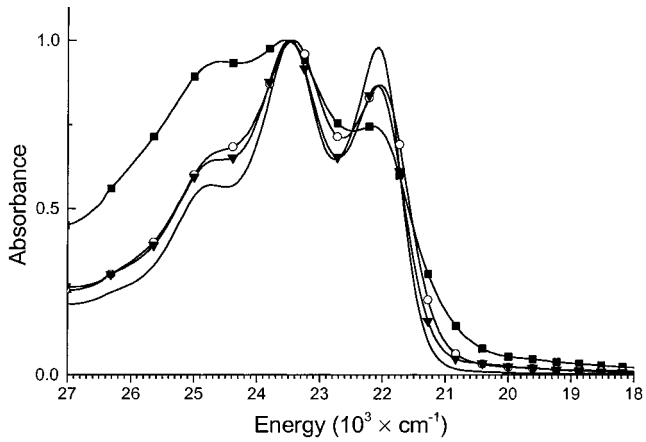

Figure 2. Comparison of absorption spectra of OPV3-modified dendrimers in 2MeTHF at T = 100 K: (−) **G0**; (▼) **G1**; (○) **G3**; (■) **G5.**

TABLE 1: Energies Associated with the Maximum of the 0−1 Vibronic Transition in Luminescence for Dendrimers of Different Generation

	SSF experiment		order statistics[a]		absorption[b]
	energy 0−1 (×10^3 cm^{-1})	ΔE (×10^3 cm^{-1})	ΔE (×10^3 cm^{-1})	ΔE (σ)	σ_{abs} (×10^3 cm^{-1})
G0	20.14	0	0	0	0.39
G1	19.70	−0.44	−0.26	−1.029	0.46
G3	19.37	−0.77	−0.44	−1.766	0.49
G5	18.63	−1.51	−0.59	−2.344	0.82

[a] Predictions for the lowest excited energy level from order statistics using eq 2. Energies relative to the average energy of the isolated chromopore, calculated using σ = 250 cm^{-1} (see text). [b] Standard deviation obtained from the fit of a Gaussian curve to the low-energy side of the 0−0 absorption band.

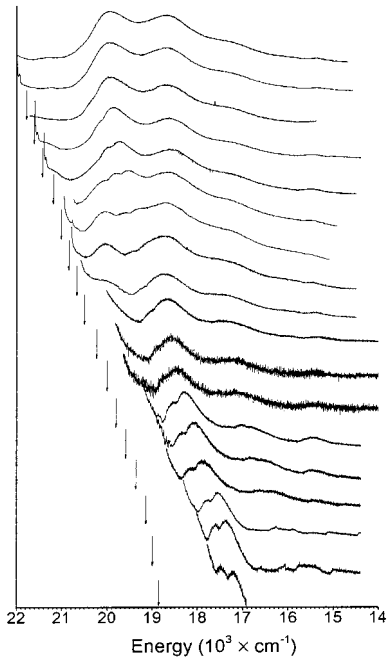

Figure 3. Site selective fluorescence spectra of **G5** in 2-MeTHF at $T = 15$ K. The arrow indicates the excitation energy.

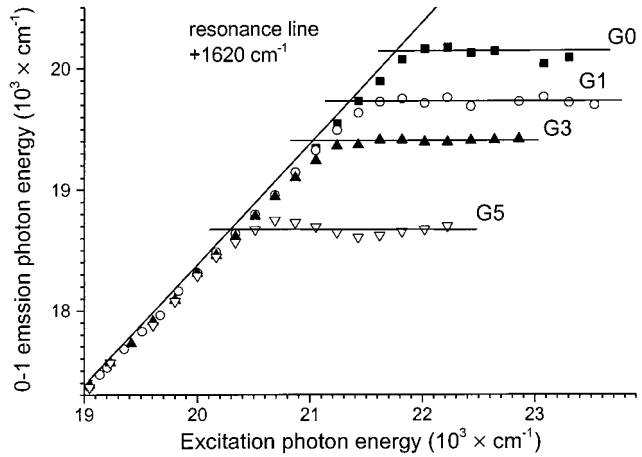

Figure 4. Analysis of the SSF spectra of dendrimers **G0**−**G5.** The energy associated with the maximum of the 0−1 vibronic transition in fluorescence spectra is plotted versus the excitation energy.

below 21.5×10^3 cm^{-1} stray light from the laser prohibits detection of the fluorescence in the 0−0 region of the spectrum. The 0−1 vibronic band can be monitored without problems. As can be seen, for lower excitation energies the 0−1 vibronic band splits into two components, one with ∼1400 cm^{-1} and another with ∼1600 cm^{-1} vibrational frequency. These two vibrational frequencies are in fact characteristic of many π-conjugated polymers.[21] Fluorescence spectra for all four dendrimers as a function of excitation wavelength have been measured and analyzed. The results are summarized in Figure 4. The position of the maximum of the 0−1 vibronic band in the SSF spectra is plotted as a function of the excitation energy. For high-energy excitation the emission is almost invariant to the excitation energy. For low excitation frequencies, however, the fluorescence spectrum shifts linearly with the excitation energy following the so-called resonance line. This behavior is to be expected when no further relaxation process in the S_1 state occurs upon excitation. Above a certain energy (E_{loc}), the position of the fluorescence bands becomes independent of the excitation frequency, indicating the onset of relaxation processes. The demarcation energies for different dendrimers are indicated by the arrows in Figure 1. They show a dependence on the dendrimer generation.

To investigate the photophysical properties further, we have performed time-resolved fluorescence measurements at low temperature. In Figure 5 results for **G0** and **G5** are shown. The fluorescence of **G0** under matrix-isolated conditions decays exponentially and has a lifetime of 1.4 ns. In liquid solution at room temperature a slightly longer lifetime is observed (1.6 ns, Figure 5C). For **G5** at low temperature, a more complicated decay of the luminescence is observed. The decay is nonexponential and short-lived components are observed. For **G5** some spectral relaxation occurs, resulting in a small time-dependent red shift of the emission. This can be seen by comparing fluorescence spectra obtained shortly after excitation and with a delay in detection (see Figure 5 B). After the delay, the 0−1 vibronic band at 18.5×10^3 cm^{-1} has broadened and its center has shifted toward lower energies by about ∼100 cm^{-1}.

Further experimental observations of the intricate photophysical behavior of the higher dendrimer generations is obtained from fluorescence measurements in the nano- to microsecond time domain. In Figure 6 fluorescence spectra for the dendrimers recorded with delayed, time-gated detection are shown. For comparison the prompt fluorescence is also shown. The behavior of **G0** is straightforward; the spectrum does not show any significant evolution with time. Emission recorded with a delay of 40 ns after excitation shows a very weak fluorescence signal at the same frequencies as observed for the ordinary fluorescenc. Given the instrumental response function of ∼10 ns, this may be interpreted as ordinary fluorescence. After 120 ns, no emission is observed. For the dendrimers of higher generation a delayed emission is observed. For **G1** this is quite weak, but for **G3** and **G5** a long-lived component is observed with a strongly red-shifted emission band (maximum at 16.5×10^3 cm^{-1}). The intensity of this component is several orders of magnitude lower than the prompt fluorescence. Its lifetime amounts to several tens of nanoseconds (∼60 ns). This emission component cannot be distinguished in the SSF spectra with time-integrated detection and selective excitation at the absorption edge. This indicates that the delayed emission most likely originates from a very minor fraction of the dendrimers.

Analysis and Discussion

We start the analysis of the spectroscopic data described above with a discussion of the SSF data shown in Figure 4. To evaluate the red shift of the emission spectrum under nonselective excitation with increasing dendrimer generation, we first make a few simplifying assumptions that help to make the problem tractable. The validity of the assumptions will then be reevaluated later on. We assume that the interchromophoric excited-state coupling energy is small compared to the width of the distribution of the excited states energies of the individual chromophoric units. Under these conditions the excitations are localized mainly on a single functional group. The energies for the lowest excited singlet state (S_1) are taken to be statistically distributed according to a Gaussian distribution (with standard deviation σ). The energies of the chromophores are assumed to be uncorrelated. We further suppose that energy transfer within the dendrimer is rapid so that fluorescence occurs from the OPV group within the dendrimer with the lowest excited-state energy (transfer complete within ∼100 ps).

To relate the energy of the lowest excited state to the number of chromophoric groups on the dendrimer (n), we calculate the

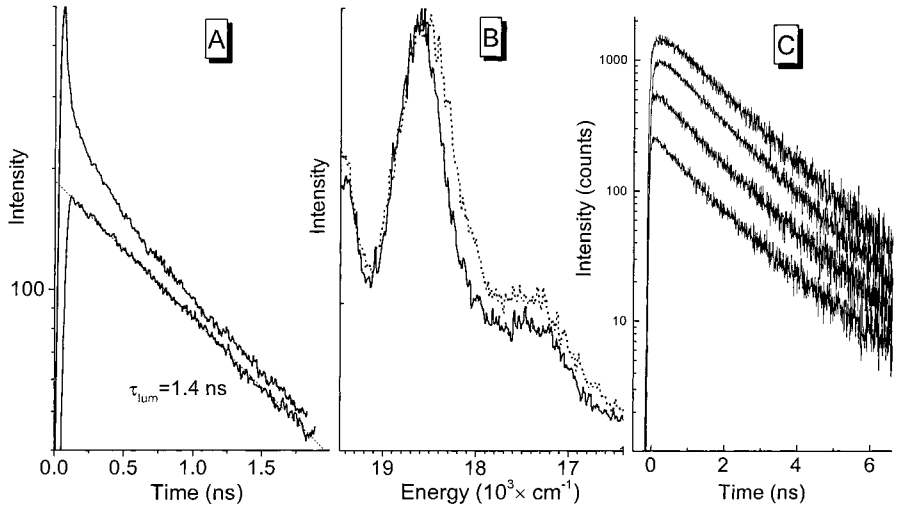

Figure 5. Time-resolved fluorescence measurements on dendrimers. (A) **G0** (lower trace) and **G5** (upper trace) in 2-MeTHF at 15 K. Excitation at 22.2 and 21.7 × 10^3 cm^{-1}, respectively. The intensity was integrated over the (19−17) × 10^3 cm^{-1} spectral region. (B) Evolution of the emission spectrum of **G5** with time at T = 15 K (see also (A)). Solid line: 0−6 ps detection window; dotted line 1.6−1.8 ns. (C) Fluorescence from (top to bottom) **G0**, **G1**, **G3**, and **G5** at room temperature in dichloromethane, excitation at 33 × 10^3 cm^{-1}, detection at 18.2 × 10^3 cm^{-1}.

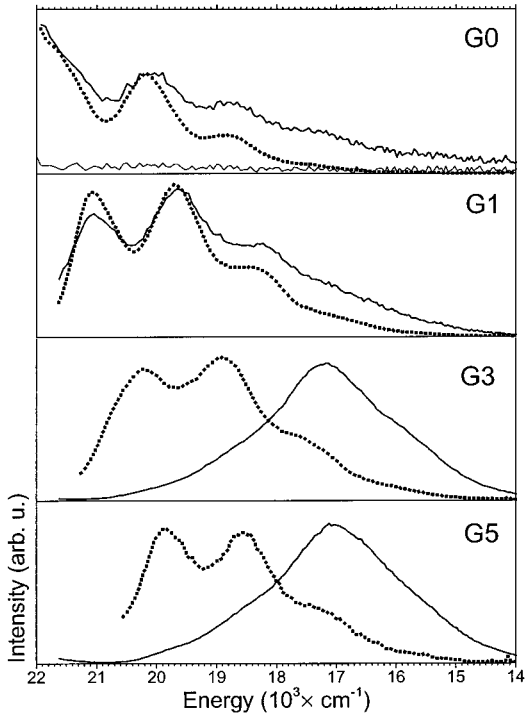

Figure 6. Delayed luminescence of dendrimers **G0**, **G1**, **G3**, and **G5** in 2-MeTHF at 77 K. The dotted line shows the prompt fluorescence. The solid line shows emission acquired in a time window opening 40 ns after the excitation and with a length of 10 μs.

expectation value (EX) of the lowest value in the set of n random samples from a parent distribution $G(x)$. This is a known problem.[22] Let $P(x)$ denote the cumulative distribution function $P(x)$ derived from $G(x)$, i.e.

$$P(x) = \int_x^{+\infty} G(x')\,\mathrm{d}x' \tag{1}$$

Then

$$\mathrm{EX}_{(n)} = \int_{-\infty}^{\infty} nx(P(x))^{n-1}\,\mathrm{d}P(x) \tag{2}$$

This formula can be generalized to cover also the expectation value for the mth moment:

$$\mathrm{EX}^m_{(n)} = \int_{-\infty}^{\infty} nx^m(P(x))^{n-1}\,\mathrm{d}P(x) \tag{3}$$

If $G(x)$ is taken as the Gaussian distribution

$$G(x) = \frac{\exp(-x^2/2\sigma^2)}{\sqrt{2\pi\sigma}} \tag{4}$$

then P(x) is related to the error function:

$$P(x) \propto 1 - \mathrm{erf}\left(\frac{x}{\sqrt{2}\sigma}\right) \tag{5}$$

To simulate the SSF data, one would also like to include a dependence on the excitation energy ϵ. This can be done as follows. We calculate the expectation value for the lowest value in the set of n samples including only values in the interval from $-\infty$ to ϵ.

$$\mathrm{EX}^m(n,\epsilon) = \frac{\int_{-\infty}^{\epsilon} x^m(P(x))^n dP(x)}{\int_{-\infty}^{\epsilon} (P(x))^n\,\mathrm{d}P(x)} \tag{6}$$

We assume that all clusters with their lowest excited state in the energy interval from $-\infty$ to ϵ can be excited with equal probability by photons of energy ϵ. Clusters with their lowest excited state above ϵ are not excited. The photon energy corresponding to the maximum of the 0−0 fluorescence band is then given by the expectation value $\mathrm{EX}^1(n,\epsilon)$ and can be calculated by numerical integration of (6). Results of these calculations are shown in Figure 7A. For nonselective high-energy excitation, a red shift of the fluorescence band is predicted with the increasing number of chromophoric groups in the dendrimer. When the excitation frequency is lowered below the expectation value of the lowest excited state, the emission energy depends quasi-linearly on the excitation energy. The exact linear dependence is obtained in the limit of very low excitation energy. In a similar way one can calculate the variance of the lowest energy levels below the excitation energy ϵ. In this way one can predict how the width of the 0−0 fluorescence band depends on n and ϵ. We also include an

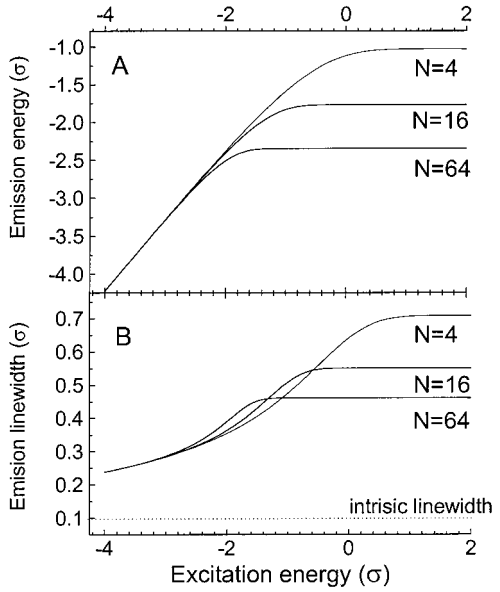

Figure 7. (A) Theoretical predictions for the energy corresponding to the maximum of the fluorescence band as a function of the energy of the excitation photons. Predictions based upon order statistics (see text) for clusters with $N = 4$, 16, and 64 chromophores, mimicking **G1**, **G3**, and **G5**. Energy unit: σ, the standard deviation of the Gaussian distribution for excited states energies of the chromophores. (B) Theoretical predictions for the width of the fluorescence band as a function of energy of the excitation photons.

intrinsic width ($\sigma_{\text{intrinsic}}$) which represents the line width of a single, isolated chromophore.

$$\text{var}(n,\epsilon) = \text{EX}^2(n,\epsilon) - (\text{EX}^1(n,\epsilon))^2 + \sigma^2_{\text{intrinsic}} \qquad (7)$$

Predictions for the width are shown in Figure 7B and were obtained by taking the square root of the variance. Under nonselective excitation with high energy one expects for **G0** a bandwidth equal to σ. For dendrimers of higher generation one predicts a narrowing of the emission bands. When the excitation energy is scanned through the absorption band, fluorescence line narrowing is predicted when exciting at the red edge.

Theoretical predictions (Figure 7A) and experiment (Figure 4) may now be compared. Qualitatively, the predicted red shift of the emission spectrum upon increasing the number of chromophores is indeed observed. For a quantitative comparison between theory and experiment we need an estimate for σ, the width of the distribution of excited-state energy for the isolated chromophores.

In Figure 8 the procedure to estimate the width of the distribution of excited-state energies is illustrated. For model compound **1** a SSF spectrum under selective excitation has been measured and the region corresponding to the 0−1 vibration is shown as dashed line in Figure 8. The spectrum is very similar to SSF spectra obtained for **G0**. For **1** we were, however, able to achieve higher resolution. For both molecules the 0−1 region actually comprises two main vibrational frequencies, 1370 and 1620 cm^{-1}. This is common for π-conjugated materials.[18] Also shown in Figure 8 is the fluorescence spectrum of **G0** at low temperature under nonselective excitation (solid line). The 0−1 band in this spectrum can be reproduced by convoluting the high-resolution SSF spectrum with a Gaussian with $\sigma = 2.5 \times 10^2$ cm^{-1} (see Figure 8). This approach to estimate σ has the advantage that a possible relaxation of the molecule in the excited state is included. For short oligomers it may be expected that due to the change in bond length alternation in the excited

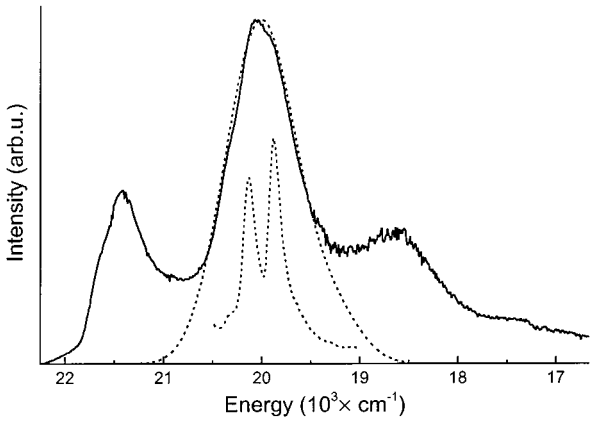

Figure 8. Determination of the inhomogeneous broadening of the fluorescence spectrum of **G0** in 2MeTHF at 15 K upon nonselective excitation (23×10^3 cm^{-1}). The dotted line with sharp peaks shows the SSF spectrum of **1**, and a convolution of this spectrum with a Gaussian with width $\sigma = 250$ cm^{-1} is also shown as a dotted line.

state, some planarization of the molecule can occur, which in turn leads to a lowering of the excited-state energy. The fact that no sharp zero phonon lines in the SSF spectra are observed provides an experimental indication for relaxation processes occurring in the excited state.

With this estimate of σ it then becomes possible to calculate the magnitude of the red shift predicted using (6). Values are listed in Table 1. The experimentally observed shifts are found to be considerably larger than predicted from theory. This discrepancy remains when one takes the value of σ as obtained from analysis of the absorption edge at 100 K (σ_{abs}; see Table 1).

Further discrepancies between experimental data and the theoretical model appear when the widths of the fluorescence bands are evaluated. Using eq 6, one predicts that the width for the fluorescence bands under nonselective excitation should decrease continuously when the number of chromophores in the cluster is increased.[23] Here rapid energy transfer to the lowest state in the cluster is assumed to take place. The predictions are illustrated in Figure 7B. The experimental data do, however, not show this trend. The width of the vibronic bands in the fluorescence actually increases slightly upon going from **G0** to **G1** and to **G3**. For **G5** a slight reduction is observed in comparison to **G3**, but the width for **G5** is certainly not smaller than for **G0**.

To account for these discrepancies, one has to reevaluate the assumption of the interactions between the chromophores being weak enough not to induce (considerable) delocalization of excitations over more than one chromophore. The other important assumption used in the analysis is that of rapid, complete energy transfer to the lowest chromophore in the cluster. Deviation from this latter assumed behavior does, however, not help to explain the discrepancy observed here. If the energy is not transferred to the chromophore with the lowest energy, then clearly the magnitude of the red shift predicted should be reduced. However, the shift predicted was already too small to match the experimental observations. We conclude that the interactions between the chromophores are nonnegligible when evaluating the energy levels of the dendritic cluster of chromophores as a whole. Further support for this conclusion comes from the time-resolved fluorescence data. These show only limited spectral diffusion in the time window investigated. This indicates that energy transfer between the OPV groups takes place on a time scale less than 10 ps and that correspond-

ingly the coupling between the chromophores has to be quite strong.

Additional evidence for the importance of interchromophoric coupling comes from the absorption spectra. The band shape of the $S_0 \rightarrow S_1$ transition changes with dendrimer generation. To explain this, the model used to derive (6) needs to be extended. An improved model, which also takes into account interchromophoric interactions, should be able to explain the following experimental observations: (1) additional reduction of the energy of the lowest excited state; (2) broadening of the distribution of the lowest excited state; (3) the position of the maximum of the 0−0 absorption band remaining at the same frequency, but the band shape of the absorption band changing; (4) rapid energy transfer between the chromophores on a time scale less than 10 ps.

Theoretical models have been developed to describe the effect of interchromophoric coupling on the properties of the excited state. These models have been used to describe the peculiar changes in band shape occurring upon aggregation of pseudoisocyanine dye molecules (formation of J or Scheibe aggregates)[24] and more recently aggregation of π-conjugated oligomers. In the latter case both changes in absorption[25−27] and emission[28,29] bands were analyzed. In these models one makes use of a Hamiltonian that includes both the excited-state interchromophoric interactions and coupling between vibrational and electronic degrees of freedom. These effects are incorporated in the model Hamiltonian (8), which has been subject of several studies.[30] In this approach one (1) neglects exchange of electrons between the molecules and (2) takes into account only one (totally symmetric) vibrational normal coordinate Q per molecule. Under these premises it is possible to calculate excited-state properties of the aggregate on the basis of parameters for a single isolated molecule without the need for quantum chemical calculations on the whole cluster of molecules.

$$H = \sum_N |N\rangle(\epsilon_N - 2\sqrt{2}\gamma Q_N)\langle N| + {Q_N}^2 + {P_N}^2 + \sum_{(N,M)} |N\rangle V_{NM}\langle M| + \text{h.c.} \quad (8)$$

In (8) $|N\rangle$ stands for the product of electronic wave functions of the molecules, all of them taken to be in their ground state, except for molecule N, which is in its first excited state. The terms ${P_N}^2$ and ${Q_N}^2$ describe the kinetic and potential energy (in units of $h\nu_{vib}/2$) of the harmonic oscillator associated with the active nuclear vibrational mode on molecule N. The terms with V_{NM} describe the transfer of the electronic excitation from molecule N to M (interchromophoric coupling).

Due to the term linear in γQ_N, the Hamiltonian cannot be written as the sum of a nuclear and electronic Hamiltonian. This term arises from Herzberg−Teller coupling of the lowest excited state with a higher excited state of the same symmetry. In the following it is assumed that the coefficient of the admixed higher state is small so that its contribution may be neglected when calculating matrix elements. As a result of the γQ term, the number of vibrational quanta is not conserved upon optical excitation of the molecule from its ground state. The electronic excitation is accompanied by a change of the equilibrium nuclear geometry. This results in a vibronic progression in absorption and emission spectra based upon the vibrational frequency of the active mode. The coupling constant γ is related to the Huang−Rhys factor S ($S = \gamma^2$), and in principle, its magnitude can be obtained by evaluation the relative intensity of the vibronic bands in absorption and emission of the *isolated* constituent molecule. If $I(0 - n)$ denotes the intensity of the nth vibronic transition, then

$$\frac{I(0-n)}{I(0-0)} = \frac{\gamma^{2n}}{n!} \quad (9)$$

Finding the eigenvalues and eigenfunctions of the Hamiltonian (8) is a nontrivial problem. The coupling between nuclear and electronic motion implies that the Born−Oppenheimer (BO) approximation does not hold. This problem is well studied.[31] Two limiting cases can be distinguished for which a simple approximate solution can be given. When V_{NM} is very large so that the γQ term can be neglected, the BO approximation applies to the aggregate as whole. In this case the distortion associated with the excitation is spread out over all the molecules involved in the excitation (large polaron). When V_{NM} is small in comparison with matrix elements of the γQ term, the BO approximation applies to the individual molecules and the distortion is limited in size to a single molecule. It migrates together with the electronic excitation through the aggregate (small polaron). For all but the purest molecular crystals, molecular materials may be regarded as disordered. In (8) disorder may be expressed by taking the site energies ϵ_N to be statistically distributed (diagonal disorder). Furthermore, disorder in the packing of the molecules leads to a spread of intermolecular coupling parameters V_{NM} (off-diagonal disorder) and also for V_{NM} a statistical distribution may be assumed.

Here we use (8) to simulate absorption and emission spectra for small clusters containing four molecules. We include both diagonal and off-diagonal disorder by choosing values for the parameters ϵ_N and V_{NM} at random from Gaussian distributions (with widths σ_d and σ_{offd}, respectively). To our knowledge the combination of electron-vibrational coupling, diagonal and off-diagonal disorder has not been considered previously. It has been recognized, however, that disorder and electron-vibrational coupling can act synergistically to induce localization of charge carriers or excitations[32] so that their combination may give rise to additional physical phenomena. Especially here where we deal with the nonrigid dendrimer core, inclusion of disorder seems important.

We use a numerical procedure to diagonalize (8) and a set of basis states that include all electronically excited states with less than five vibrational quanta is used. To illustrate the set of basis state we write (10).

$$|N;0\rangle$$
$$|N;p=1\rangle,|N;p=1,q=1\rangle,|N;p=1,q=1,r=1\rangle,|N;p=1,q=1,r=1,s=1\rangle$$
$$|N;p=2\rangle,|N;p=2,q=1\rangle,|N;p=2,q=1,r=1\rangle$$
$$|N;p=3\rangle,|N;p=3,r=1\rangle$$
$$|N;p=4\rangle \quad (10)$$

Here N denotes the index of the electronically excited molecule (1, 2, 3, or 4) and p, q, r, s the index of the molecules hosting one or more vibrational quanta (indicated by the numbers). Double electronic excitations are not taken into account. The number of singly excited states with ≤ b vibrational quanta in an aggregate with a molecules is given by

$$\frac{(a+b)!a}{a!b!} \quad (11)$$

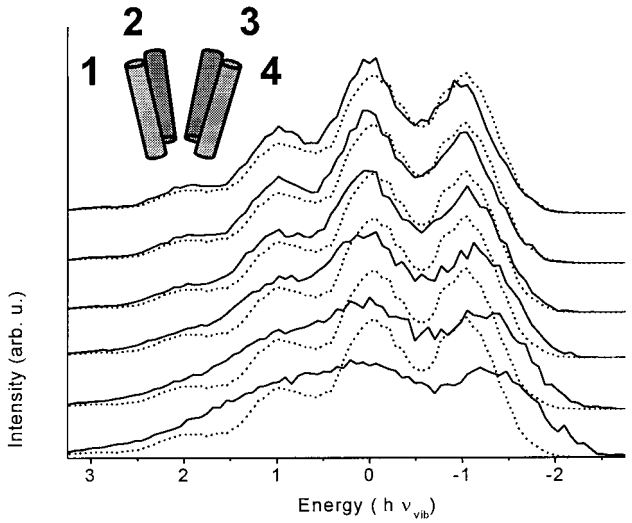

Figure 9. Theoretical modeling of the absorption spectra of a cluster of four chromophores using the Hamiltonian (8) with fixed degree of diagonal disorder and varying degree of off-diagonal disorder. The dashed lines show the simulated spectrum for isolated chromophores with their zero order excitation energy drawn from a Gaussian distribution with $\sigma = {}^1/_3$. Excited-state interchromophoric coupling energies V_{ij} are given by ${}^1/_{20}(1 + a)$, where a is drawn from a Gaussian distribution with (from top to bottom) $\sigma = 0$, 2, 4, 6, 8, and 10. All energies are in units of $h\nu_{\text{vib}}$, the vibrational quantum of the active vibration. Spectra represent an average over 2000 clusters. For all spectra, the zero on the energy scale is defined by energy associated with the pure electronic transition (vertical excitation) of the isolated OPV chromophore.

This amounts to 280 for $a = 4$ molecules and $b = 4$ vibrational quanta. Due to the rapidly increasing number of states, we were not able to simulate properties of the higher generation dendrimers of higher generations. In our calculation the four molecules making up the aggregate were placed in such a way that their centers are on the corners of a square. They are slightly tilted so that the aggregate as a whole has the shape of a cone with the main axis of the molecules making an angle of 20° with the axis of the cone. The transition dipole moment for the S_0-S_1 transition is taken parallel to the main axis of the molecules. In our case where the coupling between chromophores is not so strong, one may improve the convergence by using basis states in which the molecule N on which the distortion resides is in the relaxed excited-state equilibrium geometry. We have set $\gamma = 1$. Gaussian distributions for the parameters ϵ_N and V_{NM} were assumed. Standard software routines for generation random numbers and diagonalization of matrixes were used.[33]

Figure 9 shows simulated absorption spectra obtained by numerical diagonalization of (8). In these calculations the distribution of ϵ_N was given a width $\sigma = {}^1/_3 h\nu_{\text{vib}}$. Various band shapes shown correspond to a varying degree of off-diagonal disorder. The distribution of V_{NM} is biased to positive values, and the average V_{NM} amounts to ${}^1/_{20} h\nu_{\text{vib}}$. The relative intensities of the various vibronic bands for the cluster are different from those observed for the monomer. For the aggregate the 0−0 intensity is slightly reduced while the 0−1 intensity has increased. This change can be adjusted by choice of the bias of V_{NM} (${}^1/_{20} h\nu_{\text{vib}}$ for the curves shown). Taking distributions for V_{NM} with higher average, the 0−0 intensity is reduced and the 0−1 intensity increases further. When no off-diagonal disorder is present (uppermost spectrum) the absorption bands are relatively sharp and their maxima are slightly shifted toward higher energies. With increasing off-diagonal disorder the bands broaden and for $\sigma_{\text{offd}} = {}^1/_5 h\nu_{\text{vib}}$ the energy of maximum absorbance has not shifted in comparison with that for the isolated molecule. For higher values of σ_{offd} the bands blur and a low-energy absorption tail appears.

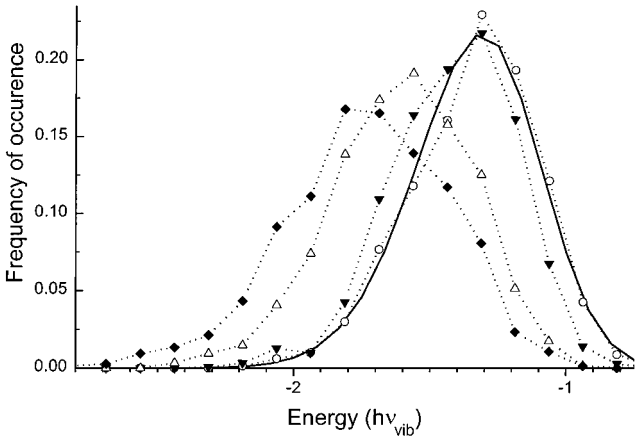

Figure 10. Distribution of the lowest excited state in clusters with four molecules (see legend Figure 9). Curves shown pertain to varying degree of off-diagonal disorder. V_{ij} is given by ${}^1/_{20}(1 + a)$, where a is drawn from a Gaussian distribution with $\sigma = 0$ (○), 4 (▼), 8 (△), and 10 (◆). The solid line shows the prediction for weakly interacting chromophores using order statistics.

Increasing off-diagonal disorder through augmenting σ_{offd} also has an effect of the probability distribution for the lowest energy level E_{low} in the cluster. This is illustrated in Figure 10. When $\sigma_{\text{offd}} = 0$ the distribution of E_{low} closely follows the prediction made with help of the order statistics (eqs 2−6). For the isolated chromophore the pure electronic energy of the photoexcited chromophore in the unrelaxed ground-state geometry (vertical excitation) is set at zero energy. The maximum of the 0−0 vibronic transition in emission then lies at $E = -1 h\nu_{\text{vib}}$ when $\gamma = 1$. This lower energy in comparison with the vertical excitation results from relaxation of the nuclear geometry.

Increasing σ_{offd} has two effects. First, the average value of E_{low} becomes lower and second, the width of the distribution for E_{low} becomes broader. From the simulations using model Hamiltonian (8) we can now draw the following conclusions. (1) The changes observed in the band shape of the $S_0 \rightarrow S_1$ transition comparing **G0** and **G1** can be qualitatively understood using (8). When the oligomer chains have a preference for aligning parallel, the higher vibronic transitions have higher intensity than for the monomer (H aggregate). (2) By including off-diagonal disorder, one can qualitatively account for the additional red shift and the width of the fluorescence band. A set of parameters that gives results compatible with the experimental observations is $\sigma_{\text{d}} \approx 5 \times 10^2$ cm^{-1}, $\sigma_{\text{offd}} \approx 5 \times 10^2$ cm^{-1}, and the average value for the coupling elements $\langle V_{NM} \rangle \approx 8 \times 10^1$ cm^{-1}. Theoretical analysis of the interaction between two distyrylbenzene molecules showed that depending upon the relative orientation of two chromophores, the coupling matrix element can have either V_{NM} positive or negative.[26] The magnitude of V_{NM} for a cofacial dimer of two molecules at the minimal intermolecular distance (4 Å) was calculated to be close to 1000 cm^{-1}.[26,27]

Finally, we discuss the delayed emission from the dendrimers. When disorder is included, the model Hamiltonian (8) predicts changes in the emission band shape occurring with time after excitation. This can be explained in the following way. Due to the disorder, the rate of excited-state decay is not the same for all clusters, nor is the fluorescence band shape. Depending on the electronic coupling between the chromophores, the intensity of the 0−0 transition relative to the 0−1 band varies. Clusters

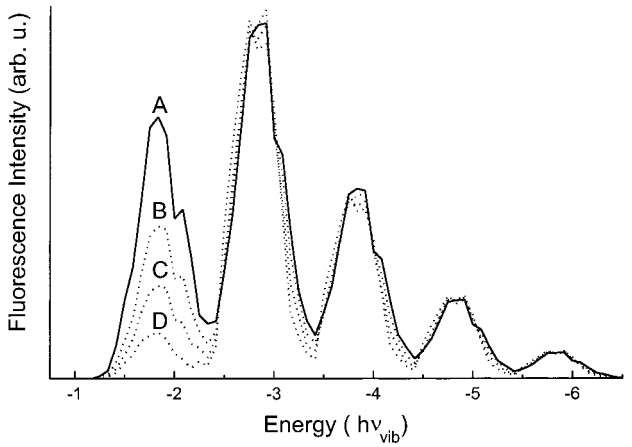

Figure 11. Simulation of the time dependence of the band shape of the emission spectrum for a cluster of four molecules using model Hamiltonian (8) (see also legend Figure 9). Diagonal disorder: site energies ϵ_N are drawn from a Gaussian distribution with $\sigma = {}^1/_3 h\nu_{vib}$. Off-diagonal disorder: V_{NM} are drawn from a Gaussian distribution with average $\mu = {}^1/_{20} h\nu_{vib}$ and width $\sigma = {}^1/_5 h\nu_{vib}$. Curve A corresponds to the time integrated fluorescence. Curves B, C, and D correspond to fluorescence in the time interval from $t = 0$ to $t = 5$, 10, and 20 times the excited-state lifetime of the isolated monomeric chromophore.

for which the 0−0 band has a low intensity generally have a low probability for radiative decay. This corresponds to the case of exciton coupling between parallel cofacial oligomers, which leads to a lower probability for the radiative decay via the 0−0 transitions[34] in comparison with the isolated molecule. The probability for the 0−1 and higher order vibronic transitions is less sensitive to electronic coupling between the chromophoric units.[28,29] Assuming that the probability for nonradiative decay is not influenced by aggregation, these clusters will have a longer emission lifetime because of the reduced probability for radiative decay. For clusters with a different arrangement of the chromophores, the probability for the 0−0 transition may be enhanced (superradiance). For such clusters the intensity of the 0−0 band relative to the 0−1 will be higher and the lifetime of the excited state should be reduced. Thus one expects for an ensemble of disordered clusters that the fluorescence at short times after excitation is dominated by the contribution from the superradiant clusters featuring a 0−0 band with high-relative intensity. At long times after excitation the contribution from the subradiant aggregates will dominate and the intensity of the 0−0 band will be reduced. This is illustrated in Figure 11, which shows model calculations of the fluorescence band shape for a cluster of four molcules obtained by numerical diagonalization of (8). Simulated spectra pertain to $t = 0$, 5, 10, and 20 times the lifetime of the isolated chromophore. The spectra are normalized. In these simulations it was assumed that the rate for nonradiative decay is the same for all clusters and the quantum yield for fluorescence from the isolated chromophores was taken to be 0.8.

In Figure 6 it can be seen that in the delayed emission from **G1** a change in the intensity of the 0−0 relative to the 0−1 band is indeed observed. This is consistent with the model calculations shown in Figure 11. However, experimentally one also observes an increase in the relative intensity of the 0−2 and higher vibronic bands. These changes are not accounted for by the model calculations. Such an increase in the intensity of higher vibronic transitions can most likely not be described by the model Hamiltonian (8). Furthermore, interchromophoric interaction as described by (8) with V_{NM} comparable in magnitude to the vibrational energy quantum can only account for a limited increase in the radiative lifetime.[28,29] The probability for the higher order vibronic transitions does not change drastically with respect to the probability for the isolated chromophore. Since the higher order vibronic transitions carry about half of the total transition probability, an increase in radiative lifetime of more than a factor of 10 cannot be accounted for by the model. Both the spectral position and the lifetime of the delayed emission indicate therefore involvement of a second excited species, e.g., an excimer or exciplex. Recently, exciplex formation between distyrylbenzene derivatives and dimethylaniline has been described.[35] In our systems exciplex formation involving OPV and the tertiary amines of the dendrimer might take place. The substitution of the distyrylbenzene with alkoxy side chains lowers the energy of the first excited state considerably and this has an unfavorable effect on the free energy for exciplex formation.

Conclusion

OPV-functionalized dendrimers provide useful and versatile model systems to investigate photophysical behavior in π-conjugated materials. Energy transfer between OPV groups and delocalization of electronic excitation over more than one chromophore can be studied. In particular we have shown that changes in the shape of the S_0-S_1 absorption band occurring with increasing dendrimer generation can be qualitatively understood in terms of coupling of the electronic motion on the chromophoric groups in the dendrimer, implying delocalization of the excitation. The inclusion of off-diagonal disorder is found to be essential to understand the experimental observations. This off-diagonal disorder could be interpreted physically in terms of a flexible dendritic core. Due to this flexibility the distances between nearest neighbor end groups and their relative orientation are not constant (as in a crystal) but are given by statistical distributions. At low temperature the conformation of the dendrimer is frozen and an ensemble of dendrimers is most probably heterogeneous with respect to conformation. The disordered arrangement of the end groups and the spread in excitation energy of the individual end groups within a dendrimer limit the extent of delocalization, and our simulations indicate that for most excited states, one particular OPV unit within in the dendrimer exists at which the excitation resides with a probability greater than 50%.

Our findings may be compared to results obtained for other mulichromophore systems. Single molecule studies on dendritic molecules with perylenecarboximide dyes have revealed heterogeneity in the spectrocopic properties of the dendrimers and the formation of "dimer-like" excited states[16a] depending upon the conformation of the denrimer core. The situation may also be compared to the B850 chlorophyl pigments in the light harvesting complex 2 of purple bacteria.[36] For this system of chromophores experimental evidence for delocalization of the exciton has been reported.[37] Also here the delocalization is limited by disorder. A major difference between the chlorophyl and OPV pigment systems is that for the former the coupling between electronic and vibrational motion can to a good approximation be neglected: The Q_y band of the bacteriochlorophyl hardly shows any vibronic fine structure. For the conjugated oligomers coupling of the electronic and vibrational motion is considerable and needs to be taken into account in order to understand the band shape of the absorption and emission spectra associated with the S_0-S_1 transition.

Acknowledgment. We gratefully acknowledge financial support from the EU LAMINATE project (S.M.), the Sonder-

forschungsbereich 383, and the Fond der Chemischen Industrie. We appreciate the support from Prof. W. W. Rühle.

References and Notes

(1) Friend, R. H.; Gymer, R. W.; Holmes, A. B.; Burroughes, J. H.; Marks, R. N.; Taliani, C.; Bradley, D. D. C.; Dos Santos, D. A.; Bredas, J. L.; Logdlund, M.; Salaneck, W. R. *Nature* **1999**, *397*, 121.

(2) Samuel, I. D. W.; Rumbles, G.; Friend, R. H. In *Primary Photoexcitations Conjugated Polymers*; Sariciftci, N. S., Ed.; World Scientific: Singapore, 1997; pp 140−173.

(3) (a) Nguyen, T. Q.; Martini, I. B.; Liu, J.; Schwartz, B. J. *J. Phys. Chem. B* **2000**, *104*, 237. (b) Jakubiak, R.; Collison, C. J.; Wan W. C.; Rothberg, L. J.; Hsieh, B. R. *J. Phys. Chem. A* **1999**, *103*, 2394. (c) Jakubiak, R., Bao Z., Rothberg, L. *Synth. Met.* **2000**, *114*, 61. (d) Blatchford, J. W.; Gustafson, T. L.; Epstein, A. J.; VandenBout, D. A.; Kerimo, J.; Higgins, D. A.; Barbara, P. F.; Fu, D. K.; Swager, T. M.; MacDiarmid, A. G. *Phys. Rev. B* **1996**, *54*, 3683. (e) Langeveld-Voss, B. M. W.; Janssen, R. A. J.; Christiaans, M. P. T.; Meskers, S. C. J.; Dekkers, H. P. J. M.; Meijer, E. W. *J. Am. Chem. Soc.* **1996**, *118*, 4908. (f) Huser, T.; Yan, M. *Synth. Met.* **2001**, *116*, 333. (g) Yan, M.; Rothberg, L. J.; Kwock, E. W.; Miller, T. M. *Phys. Rev. Lett.* **1995**, *75*, 1992. Yan, M.; Rothberg, L. J.; Papadimitrakopoulos, F.; Galvin, M. E.; Miller, T. M. *Phys. Rev. Lett.* **1994**, *72*, 1104.

(4) (a) Köhler, A.; Grüner, J.; Friend, R. H.; Müllen, K.; Scherf, U. *Chem. Phys. Lett.* **1995**, *243*, 456. (b) Lemmer, U.; Heun, S.; Mahrt, R. F.; Scherf, U.; Hopmeier, M.; Siegner, U.; Goebel, E. O.; Müllen, K.; Bässler, H. *Chem. Phys. Lett.* **1995**, *240*, 373.

(5) (a) Avgin, I.; Huber, D. L. *Phys. Rev.* B **1999**, *60*, 7646 (b) Inue, M.; Trugman, S. A.; Abrahams, E. *Phys. Rev.* B **1994**, *49*, 3190 (c) Fidder, H.; Knoester, J.; Wiersma, D. A. *J. Chem. Phys.* **1991**, *95*, 7880.

(6) (a) Hayes, G. R.; Samuel, I. D. W.; Phillips, R. T. *Phys. Rev.* B. **1997**, *56*, 3833. (b) Lemmer, U.; Göbel E. O. In *Primary Photoexcitations in Conjugated Polymers*; Sariciftci, N. S., Ed.; World Scientific: Singapore, 1997; p 211. (c) Meskers, S. C. J.; Hübner, J.; Oestreich, M.; Bässler, H. *Chem. Phys. Lett.* **2001**, *339*, 223.

(7) Bosman, A. W.; Janssen, H. M.; Meijer, E. W. *Chem. Rev.* **1999**, *99*, 1665.

(8) Schenning, A. P. H. J.; Peeters, E.; Meijer E. W. *J. Am. Chem. Soc.* **2000**, *112*, 4489.

(9) (a) Gierschner, J.; Egelhaaf, H.-J.; Oelkrug, D. *Synth. Met.* **1997**, *84*, 529. (b) Egelhaaf, H.-J. Gierschner, J. Oelkrug, D. *Synth. Met.* **1996**, *83*, 221. (c) Lane, P. A.; Mellor, H.; Martin, S. J.; Hagler, T. W.; Bleyer, A.; Bradley, D. D. C. *Chem. Phys.* **2000**, *257*, 41.

(10) Verdal, N.; Godbout, J. T.; Temur, T. L.; Bartholomew, G.; Bazan, G. C.; Kelley, A. M. *Chem. Phys. Lett.* **2000**, *320*, 95.

(11) Bazan, G. C.; Oldham, W. J.; Lachicotte, R. J.; Tretiak, S.; Chernyak, V.; Mukamel, S. *J. Am. Chem. Soc.* **1998**, *120*, 9188.

(12) Bartholomew, G. P.; Bazan, G. C. *Acc. Chem. Res.* **2001**, *34*, 30.

(13) (a) Ben-Avraham, D.; Schulman, L. S.; Bossman, S. H.; Turro, C.; Turro, N. J. *J. Phys. Chem. B* **1998**, *102*, 5088 (b) Bo, Z.; Zhang, W.; Zhang, X.; Zhang, C.; Shen, *J. Macromol. Chem. Phys.* **1998**, *199*, 1323. (c) Cardona, C. M.; Alvarez, J.; Kaifer, A. E.; McCarley, T. D.; Pandey, S.; Baker, G. A.; Bonzagni, N. J.; Bright, F. V. *J. Am. Chem. Soc.* **2000**, *122*, 6139. (d) Gopidas, K. R.; Leheny, A. R.; Caminati, G.; Turro, N. J.; Tomalia, D. A. *J. Am. Chem. Soc.* **1991**, *113*, 7335. (e) Jockusch, S.; Turro, N. J.; Tomalia, D. A. *Macromolecules* **1995**, *28*, 7416. (f) Jockusch, S.; Turro, N. J.; Tomalia, D. A. *J. Inf. Recording* **1996**, *22*, 427. (g) Jockusch, S.; Ramirez, J.; Sanghvi, K.; Nociti, R.; Turro, N. J.; Tomalia, D. A. *Macromolecules* **1999**, *32*, 4419. (h) Junge, D. M.; McGrath, D. V. *Chem. Commun.* **1997**, 857. (i) Newkome, G. R.; Narayanan, V. V.; Godinez, L. A.; Perez-Cordero, E.; Echegoyen, L. *Macromolecules* **1999**, *32*, 6782. (j) Plevoets, M.; Vögtle, F.; De Cola, L.; Balzani, V. *New J. Chem.* **1999**, *63*, 1. (k) Tabakovic, I.; Miller, L. L.; Duan, R. G.; Tully, D. C.; Tomalia, D. A. *Chem. Mater.* **1997**, *9*, 736. (l) Thornton, A.; Bloor, D.; Cross, G. H.; Szablewski, M. *Macromolecules* **1997**, *30*, 7600. (m) Yokoyama, S.; Nakahama, T.; Otomo, A.; Mashiko, S. *J. Am. Chem. Soc.* **2000**, *122*, 3174. (n) Balzani, V.; Ceroni, P.; Gestermann, S.; Kauffmann, C.; Gorka, M.; Vögtle, F. *Chem. Commun.* **2000**, 853. (o) Vögtle, F.; Gestermann, S.; Kauffmann, C.; Ceroni, P.; Vicinelli, V.; De Cola, L.; Balzani, V. *J. Am. Chem. Soc.* **1999**, *121*, 12161. (p) Tsuda, K.; Dol, G. C.; Gensch, T.; Hofkens, J.; Latterini, L.; Weener, J. W.; Meijer, E. W.; De Schryver, F. C. *J. Am. Chem. Soc.* **2000**, *122*, 3445. (q) Yeow, E. K. L.; Ghiggino, K. P.; Reek, J. N. H.; Crossley, M. J.; Bosman, A. W.; Schenning, A. P. H. J.; Meijer, E. W. *J. Phys. Chem. B* **2000**, *104*, 2596.

(14) (a) Balzani, V.; Campagna, S.; Denti, G.; Juris, A.; Serroni, S.; Venturi, M. *Acc. Chem. Res.* **1998**, *31*, 26. (b) Adronov, A.; Gilat, S. L.; Fréchèt, J. M. J.; Ohta, K.; Neuwahl, F. V. R.; Fleming, G. R. *J. Am. Chem. Soc.* **2000**, *122*, 1175. (c) Gilat, S. L.; Adronov, A.; Fréchèt, J. M. J. *Angew. Chem., Int. Ed. Engl.* **1999**, *38*, 1422. (d) Swallen, S. F.; Zhu, Z.; Moore, J. S.; Kopelman, R. *J. Phys. Chem. B* **2000**, *104*, 3988. (e) Stewart, G. M.; Fox, M. A. *J. Am. Chem. Soc.* **1996**, *118*, 4354. (f) Balzani, V.; Ceroni, P.; Gestermann, S.; Gorka, M.; Kauffmann, C.; Maestri, M.; Vögtle, F. *Chem. Phys. Chem.* **2000**, *1*, 224. (g) Devadoss, C.; Bharathi, P.; Moore, J. S. *J. Am. Chem. Soc.* **1996**, *118*, 9635. (h) BarHaim, A.; Klafter, J.; Kopelman, R *J. Am. Chem. Soc.* **1997**, *119*, 6198.

(15) (a) L. A. Baker, R. M. Crooks *Macromolecules* **2000**, *33*, 9034. (b) Wilken, R.; Adams, J. *Macromol. Rapid Commun.* **1997**, *18*, 659. (c) Vitukhnovsky, A. G.; Sluch, M. I.; Krasovskii, V. G.; Muzafarov, A. M. *Synth. Met.* **1997**, *91*, 375. (d) Sluch, M. I.; Scheblykin, I. G.; Varnavsky, O. P.; Vitukhnovsky, A. G.; Krasovskii, V. G.; Gorbatsevich, O. B.; Muzafarov, A. M. *J. Lumin.* **1998**, *76−77*, 246.

(16) (a) Hofkens, J.; Maus, M.; Gensch, T.; Vosch, T.; Cotlet, M.; Köhn, F.; Herrmann, A.; Müllen, K.; De Schryver, F. C. *J. Am. Chem. Soc.* **2000**, *122*, 9278. (b) Karni, Y.; Jordens, S.; De Belder, G.; Hofkens, J.; Schweitzer, G.; De Schryver, F. C.; Herrmann A.; Müllen, K. *J. Phys. Chem. B* **1999**, *103*, 9378. (c) De Belder, G.; Schweitzer, G.; Jordens, S.; Lor, M.; Mitra, S.; Hofkens, J.; De Feyter, S.; Van der Auweraer, M.; Herrmann, A.; Weil, T. Müllen, K.; De Schryver, F. C. *Chem. Phys. Chem.* **2001**, *2*, 49. (d) Maus, M.; Mitra, S.; Lor, M.; Hofkens, J.; Weil, T.; Herrmann, A.; Müllem, K.; De Schryver, F. C. *J. Phys. Chem. A* **2001**, *105*, 3961.

(17) Personov, R. I. In *Spectroscopy and Excitation Dynamics of Condensed Molecular Systems*; Agranovich, V. M., Hochstrasser, R. M., Eds.; North-Holland: Amsterdam, 1983; p 555.

(18) Bässler, H.; Schweitzer, B. *Acc. Chem. Res.* **1999**, *32*, 173.

(19) Peeters, E.; Marcos, A.; Meskers, S. C. J.; Janssen, R. A. J. *J. Chem. Phys.* **2000**, *112*, 9445.

(20) Scholes, G. D.; Larsen, D. S.; Fleming, G. R.; Rumbles, G.; Burn, P. L. *Phys. Rev. B* **2000**, *61*, 13670.

(21) Bässler, H.; Schweitzer, B. *Acc. Chem. Res.* **1999**, *32*, 173.

(22) David, H. A. *Order Statistics*; Wiley: New York, 1970.

(23) Morgan, J. R.; El-Sayed, M. A. *J. Phys. Chem.* **1983**, *87*, 383.

(24) Kobayashi, T. *J-aggregates*; World Scientific: Singapore, 1996.

(25) Manas, E. S.; Spano, F. C. *J. Chem. Phys.* **1998**, *109*, 8087.

(26) Siddiqui, S.; Spano, F. C. *Chem. Phys. Lett.* **1999**, *308*, 99.

(27) Spano, F. C.; Siddiqui, S. *Chem. Phys. Lett.* **1999**, *314*, 481.

(28) Spano, F. C. *Chem. Phys. Lett.* **2000**, *331*, 7. (b) Spano, F. C. *Synth. Met.* **2001**, *116*, 339.

(29) Meskers, S. C. J.; Janssen, R. A. J.; Haverkort, J. E. M.; Wolter, J. H. *Chem. Phys.* **2000**, *260*, 415.

(30) (a) Lu, N.; Mukamel, S. *J. Chem. Phys.* **1991**, *95*, 1588. (b) Scherer, P. O. J. *Adv. Mater.* **1995**, *7*, 451.

(31) (a) Förster, Th. In *Modern Quantum Chemistry part III*; Sinanoglu, O., Ed.; Academic Press: New York, 1965; p 93. (b) Simpson, W. T.; Peterson, D. L. *J. Chem. Phys.* **1957**, *26*, 588. (c) McRae, E. G. *Aust. J. Chem.* **1961**, *14*, 354. (d) Siebrand, W. *J. Chem. Phys.* **1964**, *40*, 2223. (e) Witkowski, A.; Mofitt, W. *J. Chem. Phys.* **1960**, *33*, 872. (f) Fulton, R. L.; Gouterman, M. *J. Chem. Phys.* **1961**, *35*, 1059.

(32) Emin, D.; Bussac, M.-N. *Phys. Rev. B* **1994**, *49*, 14290.

(33) Press: W. H.; Flannery, B. P.; Teukolsky, S. A.; Vetterling, W. T. *Numerical Recipes*; Cambridge University Press: Cambridge, 1986.

(34) Cornil, J. dos Santos, D. A. Crispin, X. Silbey, R.; Brédas J. L. *J. Am. Chem. Soc.* **1998**, *120*, 1289.

(35) Wang, S.; Bazan, G. C. *Chem. Phys. Lett.* **2001**, *333*, 437.

(36) Sundström, V.; Pullerits, T.; van Grondelle, R. *J. Phys. Chem. B* **1999**, *103*, 2327.

(37) (a) Ketelaars, M.; van Oijen, A. M.; Matsushita, M.; Köhler, J.; Schmidt, J.; Aartsma, T. J. *Biophys. J.* **2001**, *80*, 1591. (b) Chachisvilis, M.; Kühn, O.; Pullerits, T.; Sundström, V. *J. Phys. Chem. B* **1997**, *101*, 7275.